Detection of obstructive sleep apnoea using dynamic filter-banked features

Article *in* Expert Systems with Applications · August 2012

DOI: 10.1016/j.eswa.2012.02.043

4 authors:

Juan David Martinez-Vargas
Instituto Tecnológico Metropolitano

Lina María Sepúlveda-Cano
Universidad de Medellín

Carlos M. Travieso
Universidad de Las Palmas de Gran Canaria

German Castellanos-Dominguez
National University of Colombia

Expert Systems with Applications 39 (2012) 9118–9128

Contents lists available at SciVerse ScienceDirect

Expert Systems with Applications

journal homepage: www.elsevier.com/locate/eswa

Detection of obstructive sleep apnoea using dynamic filter-banked features ☆

J.D. Martínez-Vargas [a,*], L.M. Sepulveda-Cano [a], C. Travieso-Gonzalez [b], G. Castellanos-Dominguez [a]

[a] Universidad Nacional de Colombia, Signal Processing and Recognition Group, Km. 9, Vía al aeropuerto, Campus La Nubia, Manizales, Colombia
[b] Universidad de Las Palmas de Gran Canaria, Technological Centre for Innovation in Communications (CeTIC), Campus Universitario de Tafira, s/n, Las Palmas de Gran Canaria, Spain

ARTICLE INFO

Keywords:
Obstructive sleep apnea
Heart rate variability
Dynamic filter-banked features
Spectral splitting

ABSTRACT

There is a need for developing simple signal processing algorithms for less costly, reliable and noninvasive Obstructive Sleep Apnoea (OSA) diagnosing. One of the promising directions is to provide the OSA analysis based on the heart rate variability (HRV), which clearly shows a non-stationary behavior. So, a feature extraction approach, being capable of capturing the dynamic heart rate information and suitable for OSA detection, remains an open issue. Grounded on discriminating capability of frequency bands of HRV activity between normal and OSA patients, features can be extracted. However, some HRV normal spectrograms resemble like pathological ones, and vice versa; so, prior to extract the feature set, the energy spatial contribution contained in each subŨband should be clarified. This paper presents a methodology for OSA detection based on a set of short-time feature banked features that are extracted from the spectrogram of the HRV time series. The methodology introduces the spectral splitting scheme, which searches for spectral components with alike stochastic behavior improving the OSA detection accuracy. Two different splitting approaches are considered (heuristic and relevance-based); both of them performing minute-by-minute classification comparable with other outcomes that are reported in literature, but avoiding more complex methods or more computed features. For validation purposes, the methodology is tested on 1-min HRV-segments estimated from 50 Physionet database recordings. Using a parallel combining *k-nn* classifier, the assessed dynamic feature set reaches as much as 80% value of accuracy, for both considered approaches of spectral splitting. Attained results can be oriented in research focused on finding alternative methods used for less costly and noninvasive OSA diagnosing with the additional benefit of easier clinical interpretation of HRV-derived parameters.

1. Introduction

Obstructive Sleep Apnoea (OSA) is one of the most common sleep pathologies with high prevalence among the general population (at least, 2% of women and 4% of men (Chervin & Burns, 2011)), and may have dangerous impact on daily living activities. Patients suffering from sleep apnea report poor mental performance and a series of physiological problems (obesity, hypertension, and arrhythmia). Diagnosis and treatment of all potential OSA syndrome patients will have a great impact on the capacity of sleep clinics and on the budget for public health care (van Houwelingen, van Uffelen, & van Vlie, 1999).

To perform an automatic OSA diagnosis, detection of repetitive episodes of apnoea and hypopnoea during sleep is carried out, mostly, by attended overnight polysomnography in a sleep laboratory. However, regarding to standard polysomnography test the following disadvantages are frequently attributed: high cost, discomfort of the electrodes connecting to the body, high amount of information required to be analyzed, and the diagnosis is typically subjective.

One of the promising directions for less costly, noninvasive, reliable and ambulatory screening is to provide the OSA analysis based on the heart rate variability (HRV), supported by early researches concluding that the events of apnoea and hypopnoea are related to concomitant cyclic variations in heart rate. HRV can provide information on the relative inputs of the two autonomic nervous system mutually antagonistic components the sympathetic one, which acts to increase heart rate, and the parasympathetic component, which acts to slow the heart and to dilate blood vessels (McMillan, 2002). The former component activity is measured by the power in the termed Low Frequency (LF) spectral band ($f \in [0.04, 0.15]$ Hz), while the latter activity is measured by high frequency (HF) band ($f \in [0.15, 0.40]$ Hz).

Although HRV spectral analysis is used to evaluate the activity of the autonomic nervous system, commonly imposed stationary assumption does not hold, since analysis framed on the HRV-derived features must deal with non-stationary signals (typical of apnoea episodes (Al-Angari & Sahakian, 2007)). In fact, there is a well-defined

☆ This document is a collaborative effort.

* Corresponding author. Tel.: +57 6 8879300x55713.
E-mail addresses: jmartinezv@unal.edu.co (J.D. Martínez-Vargas), lmsepulvedac@unal.edu.co (L.M. Sepulveda-Cano), ctravieso@dsc.ulpgc.es (C. Travieso-Gonzalez), cgcastellanosd@unal.edu.co (G. Castellanos-Dominguez).

0957-4174/$ - see front matter © 2012 Elsevier Ltd. All rights reserved.
doi:10.1016/j.eswa.2012.02.043

research direction, with a rich and controversial history, investigating whether the normal heart activity is chaotic or not (Glass, 2009). So, different time–frequency (t–f) and time-varying approaches have been proposed with the aim to track the modification of the HRV spectra during ischaemic attacks, provocative stress testing, sleep or daily-life activities (Mainardi, 2009). Furthermore, grounded on discriminating capability of frequency bands of HRV activity between normal and sleep apnoea patients, spectral sub-band methods are becoming more popular for feature extracting t–f techniques. But often all the extracted features from enhanced t–f representations are analyzed by static statistical approach, and hence missing a valuable information about the time-evolving HRV process. Accordingly, extracted data might be processed as stochastically dependent, and thus, there is a need for a feature extraction approach being capable of capturing the dynamic information. Along with static filter-banked features that take energy values by using splitting scheme over t–f representations, short-time filter-banked features are derived to give robust estimate of the overall temporal behavior of HRV signal with the additional benefit of easier clinical interpretation. Particularly, in (Curcie & Craelius, 1997), it is assumed that specific heart rate patterns are characteristic of individuals that can be described with cepstral vectors. Although, increasing number of filter-banked features should produce greater spectral resolution, the proper choice of number of features as well as the number of filters used to compute the coefficients turn out to be a compromise between information vs. consistency of the feature set estimation. In addition, there are some HRV normal t–f representations whose waveform resembles like pathological ones, and vice versa; so, prior to extract the feature set, the energy spatial contribution contained in each sub-band should be clarified. Therefore, frequency sub-band selection is to be carried out to optimize the performance of the spectral splitting algorithm in terms of improving the highest OSA detection accuracy.

This paper presents a methodology for OSA detection based on a set of short-time feature banked features that are extracted from the spectrogram of the HRV time series. The methodology introduces the spectral splitting concept, which searches for spectrogram spectral components with alike dynamic behavior improving the highest OSA detection accuracy. To this end, two different multi-band splitting approaches are considered (heuristic and relevance-based); both of them performing accuracy comparable with another outcomes, reported in the literature. Attained results can be oriented in research focused on finding alternative methods used for less costly and noninvasive OSA diagnosing with the additional benefit of easier clinical interpretation of HRV-derived parameters. The rest of this paper is organized as follows: generation of dynamic filter-banked features is introduced in Section 2, including a detailed explanation of considered approaches of multi-band splitting. Next, the proposed methodology for automatic OSA detection is developed in Section 3 that is based on a set of short-time feature banked features, which are extracted from the spectrogram of the HRV time series. Discussion of the results as well as regarding conclusions are given in Sections 4 and 5, respectively.

2. Materials and methods

2.1. Generation of dynamic filter-banked features

In this study, OSA detection is conducted by using the set of short-time filter-banked features $\{\boldsymbol{x}_n \in \mathbb{R}^{1\times T}\}$. Such a measurement can be extracted from a given t–f representation of input HRV signal, since it is inherently a time-evolving spectral representation. In particular, the short time Fourier Transform is used introducing a time localization concept by means of a tapering window function of short duration, ϕ, that is going along the underlying HRV signal, $y(t)$, i.e.,

$$\boldsymbol{S}_y(t,f) = \left| \int_T y(\tau)\phi(\tau - t)e^{-j2\pi f\tau}d\tau \right|^2, \ \boldsymbol{S}_y(t,f) \in \mathbb{R}^+ \tag{1}$$

with t, $\tau \in T$, $f \in F$.

Based on introduced *spectrogram* of Eq. (1), the corresponding t–f representation matrix, $\boldsymbol{S}_y \in \mathbb{R}^{T\times F}$, can be described by the row vectors, $\boldsymbol{S}_y = [\boldsymbol{s}_1 \ldots \boldsymbol{s}_f \ldots \boldsymbol{s}_F]^{\top p}$, with $\boldsymbol{s}_f \in \mathbb{R}^{1\times T}$, where vector $\boldsymbol{s}_f = [s(f,1) \ldots s(f,t) \ldots (f,T)], s(f,t) \in \mathbb{R}$, is each one of the time-variant spectral decomposition component at frequency f, and equally sampled through the time axis t.

Within the context of feature extraction, a filter-bank divides the spectrogram into bands and is defined by the number of filters, the shape, centre frequency and bandwidth of each filter. Regarding the determination of those parameters, the multi-band scheme can be performed which splits the whole frequency range F of the spectrogram of Eq. (1) into several sub-bands $\{\Delta F_n\}$, comprising a set of adjacent spectral components $\{\boldsymbol{s}_f\}$, from where time-variant features are to be extracted independently. That is, each assessed frequency sub-band ΔF_n, from end to end along the time domain, holds the boundary within a single dynamic feature $\boldsymbol{x}_n$ is calculated.

For the sake of simplicity, present study performs the set of filter-banked *Frequency Cepstral Coefficients* (FCCs) for generation of dynamic features, extracted from the enhanced t–f representation in hand. Although other filter-banked based approaches might be also considered, as discussed in (Sepulveda-Cano, Gil, Laguna, & Castellanos-Dominguez, 2011). So, given a discrete time series, $y(t)$, being the sampled version of a continuous HRV signal, each FCC coefficient around time t is extracted by discrete cosine transform of triangular log-shape filter banks, $\{\delta F_m(f): f \in \Delta F_n\}$, spaced in the frequency domain:

$$x_n(t) = \sum_{m \in n_F} \log(\tilde{s}_m(t)) \cos\left(n\left(m - \frac{1}{2}\frac{\pi}{p}\right)\right) \tag{2}$$

where $n \in p$ with p the number of desired dynamic FCC features to be considered, and $s_m(t)$ is the weighted sum of each frequency filter response set, i.e.,

$$\tilde{s}_m(t) = \sum_{f \in \Delta F_n} s(f,t)\delta F_m(f),$$

being $m \in n_F$, t, and f the indexes for filter ordinal, time, and frequency axes, respectively.

2.2. Multi-band splitting upon estimated spectrogram

Within the framework of the filter-banked feature extraction, estimation of both the number of dynamic features p as well as the number of filter banks n_F is provided by using the above explained cepstral partition (see Eq. (2)) upon the given spectrogram (see Eq. (1)). At this point, it should be remarked that the main purpose of the present work is to optimize the performance of the spectral splitting algorithm in terms of improving the highest OSA detection accuracy, but with the lowest possible complexity, i.e., with the fewest number of stochastic features p and without increasing the computational effort.

In addition, either way of spectral splitting over spectrograms should be carried out separately for both considered HRV bands of interest (LH and HF), because of their markedly different statical behavior.

Since every vectorial feature is attained by multi-band splitting modeling, the spectrogram spectral partition set for each bandwidth of interest can be determined by one of the following approaches:

i. *Heuristic splitting:* To obtain information about the energy distribution, a given bandwidth of interest is arbitrary split in equally spaced sub-band partitions, $\{\Delta F_n\}$. So, a linear grid is used, based on a regular partition in the spectrogram frequency axis. To provide sufficient information related to the non-stationary properties of the HRV signal, from every sub-band partition a single dynamic feature is calculated, by using short-time representation of the signal fractional energy in a specific frequency sub-band and time window. Next, the underlying idea is to search for an optimal dynamic feature set by exploring all the suitable combinations between the filter bank number n_F and the feature amount p. With this in mind, an iterative searching process takes place by which the sub-band partition set in hand is stepwise increased. At the beginning, a given bandwidth of interest is split in two halves, conforming the initial sub-band partition set. Therefore, two corresponding FCC dynamic features are estimated. A given performance measure is accomplished for every combination of extracted dynamic features. The proper filter bank number per single feature is empirically fixed to be one. During the next step, a sub-band set is augmented in one element, and now the spectrogram is split in three regular partitions. Next step includes a four regular partition set, and so on. The procedure is done unless the best evaluation measure overcomes a given threshold ϵ. The resulting amount of p providing the best performance is selected as the optimal number of dynamic filter-banked features.
ii. *Relevance-based splitting:* Nevertheless, the above explained heuristic splitting approach does not take advantage of the information about the irregular energy spatial distribution of the spectrogram. In fact, it would be desirable to accomplish sub-band partitions enclosing spectral components with alike time-evolving behavior (i.e., holding similar information). To this purpose, the sub-band partition set can be determined by introducing the concept of *Stochastic Variability* measuring the amount of useful information for OSA detection within every spectral component. So, the higher measured variability the more relevant spectral component for OSA detection.

In this study, an unsupervised measure of time-variant relevance is assessed. Specifically, the time-evolving principal component analysis is extended to the dynamic feature modeling by stacking the input observation matrix in the following manner:

$$\Xi_y = \begin{bmatrix} \boldsymbol{s}_1^1 & \boldsymbol{s}_2^1 & \cdots & \boldsymbol{s}_F^1 \\ \boldsymbol{s}_1^2 & \boldsymbol{s}_2^2 & \cdots & \boldsymbol{s}_F^2 \\ \vdots & \vdots & \vdots & \vdots \\ \boldsymbol{s}_1^M & \boldsymbol{s}_2^M & \cdots & \boldsymbol{s}_F^M \end{bmatrix}, \Xi_y \in \mathbb{R}^{M\times FT} \tag{3}$$

where vector $\boldsymbol{s}_f^i$ corresponds to fth short-term spectral component estimated from the ith spectrogram matrix, $\boldsymbol{S}_y^i$, which is related to the ith object, with $i \in M$.

Consequently, the amount of stochastic variability of the spectral component set is accomplished by calculating the singular value decomposition over observation matrix in Eq. (3). So, the following time-variant relevance measure is carried out (Sepulveda-Cano et al., 2011):

$$\boldsymbol{g}(\Xi_y;\tau) = [\chi(1)\cdots\chi(\tau)\cdots\chi(FT)]^{\top p}, \boldsymbol{g}(\Xi_y;\tau) \in \mathbb{R}^{FT\times 1} \tag{4}$$

being $\chi(\tau) = E\left\{|\lambda_f^2 \upsilon_f(\tau)| : \forall f \in F\right\}$, where $\{\lambda_f\}$ is the relevance eigenvalue set of matrix Ξ_y, and scalar-valued $\upsilon_f(\tau)$ is the respective element at τ moment, with $\tau = 1, \ldots, FT$ that indexes every one of the relevance values computed for the whole time-variant data set. Notation $E\{\cdot\}$ stands for the expectation operator.

To determine distinctly the relevance related to each one of the time-variant spectral components, measure vector given in Eq. (4) can be rearranged into a matrix, termed *relevance matrix*, as follows:

$$\boldsymbol{G}(\boldsymbol{S}_y) = [\boldsymbol{g}(\Xi_y;1,t)\cdots\boldsymbol{g}(\Xi_y;f,t)\cdots\boldsymbol{g}(\Xi_y;F,t)]^{\top}, \boldsymbol{G}(\boldsymbol{S}_y) \in \mathbb{R}^{T\times F} \tag{5}$$

where every row corresponds to a sectioned version of vector $\boldsymbol{g}(\Xi_y;\tau)$, defined as:

$$\boldsymbol{g}(\Xi_y;f,t) = [\chi((f-1)T+1)\ldots\chi(t)\ldots\chi(fT)], \boldsymbol{g}(\Xi_y;f,t) \in \mathbb{R}^{T\times 1} \tag{6}$$

So, vector $\boldsymbol{g}(\Xi_y; f,t)$ in Eq. (6) plainly holds the respective contribution of the time-variant spectral component $\boldsymbol{s}_f$ along the fixed moments of time. Therefore, to summarize the contribution of a single spectral component, a simple average is accomplished, i.e.,

$$g(\boldsymbol{s}_f) = \boldsymbol{E}\{\boldsymbol{g}(\Xi_y;f,t) : \forall t\}, \quad g(\boldsymbol{s}_f) \in \mathbb{R}$$

Fig. 1 illustrates the stepwise implementation of the time-evolving principal component analysis, which is extended for achieving the spectrogram splitting based on the stochastic variability measure of the spectral component set.

At the end of the multivariate procedure (see Fig. 1a), a vector $\gamma(f) = [g(\boldsymbol{s}_1)\ldots\ g(\boldsymbol{s}_f)\ldots g(\boldsymbol{s}_F)]$, is achieved that contains stochastic variability measured for the whole spectral component set, $\{\boldsymbol{s}_f\}$. Due to the low-pass restriction inherently to HRV time series, then it should be assumed a high correlation level between every single pair of adjacent spectral components $\{\boldsymbol{s}_f, \boldsymbol{s}_{f+1}: \forall f \in \Delta F\}$, consequently, those frequencies where the measured stochastic variability gets a local minima along the frequency axis, i.e., $\min_{\forall f}\{\gamma(f)\}$, should be considered as good candidates of boundaries of the searched sub-band partition set, $\{\Delta F_n\}$, as outlined in SubFig. 1b.

It must be noted that the main difference between both considered splitting approaches is given in terms of the relevance measure needed for feature selection. In case of heuristic approach, the measure is of wrapper type and corresponds to the OSA accuracy, while the second approach uses a filter measure that is based on stochastic variability.

3. Experimental setup

Supported on the set of extracted filter-banked dynamic features, the proposed methodology for automatic OSA detection appraises the next stages: (a) preprocessing, (b) t–f representation enhancement, (c) Filter-bank feature generation based on multi-band spectral splitting, and (d) OSA detection.

Fig. 2 shows the experimental outline of OSA detection and the methods subject to investigation. Testing of proposed methodology is carried out on dynamic features that are calculated for HRV time series, which is computed from electrocardiographic recordings (ECGs).

3.1. Electrocardiographic recording database

The analyzed data come from the public Physionet database (www.physionet.org). The whole-night ECG recordings contain all the events that occur during a night including apnoeas, arousals, movements, and also some wakefulness episodes. Every one of apnoea events was labeled either as obstructive or mixed. One-min segments containing hypopnoea were also scored as apnoea events. Apnoea scoring was carried out on the basis of standard criteria by an expert sleep clinician. The subjects in the Physionet database were classified into three classes: A, B, and C. A recordings is regarded to class A (Apnoea) if it contains, at least, one hour with an apnoea index of 10 or more, and at least 100 apnoea episodes.

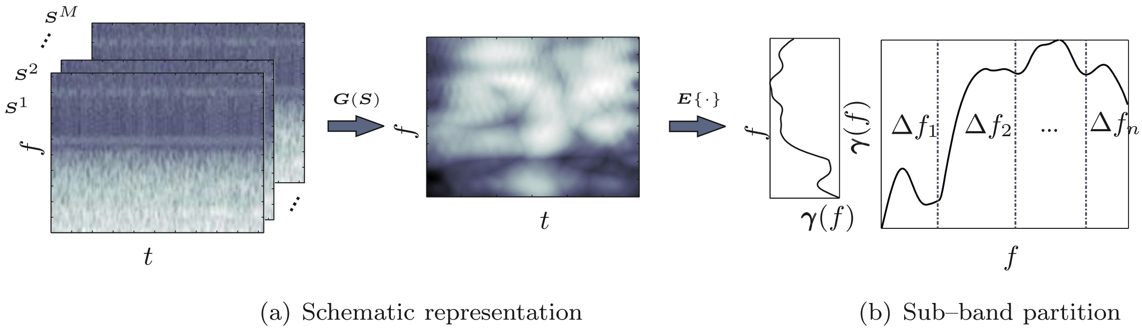

Fig. 1. Time-evolving principal component analysis extended to the spectral component modeling for multi-band splitting.

The class A subjects were fifteen men and one woman, with a mean age of 50 years (29–63). A recording is regarded to class B (termed borderline) if it contains, at least, one hour with an apnoea index of 5 or more, and between 5 and 99 min with apnoea. Recordings containing fewer than 5 min of disordered breathing were put in the normal (control, or class C) group. The C group consisted of six male and five female subjects with a mean of 33 years (27–42) (Haitham, Angari, & Sahakian, 2007).

Although the whole Physionet database contains a total of 70 ECG signals, the learning set for present study holds only 50 recordings that are selected in accordance with (Mendez et al., 2010). Particularly, database ECG signals with a large number of ectopic beats (more than 10% of the beats within the recording length) are not included in the present research. So, 25 recordings are chosen to be used as a classification training set, whereas a second group with the other 25 recordings is used as a validation set. As a result, the training set consists of 4950 apnoeic 1-min segments and 7127 non-apnoeic 1-min segments, while the testing set holds 4428 apnoeic and 7927 non-apnoeic 1-min segments.

3.2. Preprocessing and t–f representation enhancement

ECG recordings are digitized at 100 Hz with 16 bit resolution. Basically, automatic OSA diagnosis requires the extraction of HRV time series from each ECG recording, which in this case can be estimated more precisely if an accurate recognition of the QRS complex fiducial points is achieved. In this work, QRS complex detection is carried out by the method proposed in (Sörnmo & Laguna, 2005), that includes linear filtering, followed by a non linear transformation, and adaptive decision rules, as well. Further smoothing of anomaly valued peaks of assembled beat-to-beat interval time series is achieved (Lado et al., 2009). Then, the HRV time series is normalized, termed $y'(t)$, as recommended in (Kudriavtsev, Polyshchuk, & Roy, 2007):

$$y'(t) = \frac{2(y(t) - \boldsymbol{E}\{\boldsymbol{y}\})}{\max_{\forall t}\{\boldsymbol{y}\} - \min_{\forall t}\{\boldsymbol{y}\}}, \quad t \in T.$$

Concrete examples of estimated HRV time series are shown in Fig. 3. In particular, Fig. 3a shows a 10-min HRV of a normal subject during sleep, while Fig. 3b shows 10-min HRV of an OSA subject, respectively. As already fixed in (Haitham et al., 2007), OSA subjects tend to have more regular HRV pattern than normal ones have.

Next, enhancement of HRV time series is carried out by using t–f representation. Thus, based on spectral HRV signal properties, the spectrogram is computed employing a sliding Hamming window with the following parameter estimation set (Sepulveda-Cano et al., 2011): 32.5 ms processing window length, 50% of overlapping, and 512 frequency bins.

As explained before, both HRV frequency bands of interest are considered for the OSA detection: LF and HF. The former band is assumed to reveal the mixture of the sympathetic and parasympathetic activity while the HF band reflects just the parasympathetic branch activity of automatic nervous system.

Nevertheless, to illustrate the difficulty of addressed problem, Fig. 4 shows few 1-min HRV segments, belonging to normal and pathological classes, along with their respective estimated spectrograms. It can be seen that there are some normal segments whose pattern resembles like pathological ones, and vice versa. Although energy of pathological representative spectrograms is concentrated around the lower frequencies, their main LF accumulation has a time-variant behavior. In turn, normal labeled t–f representations display more active HF components, but with patterns changing also along the time.

3.3. Feature extraction by spectral splitting scheme

This section discusses in detail the implementation of the investigated spectrogram splitting approaches as previous step for dynamic filter-banked feature generation.

Discussed multi-band scheme is carried out by one of the following approaches: (i) heuristic and (ii) relevance-based.

3.3.1. Heuristic approach

To get an optimal linear grid of sub-band partitions over each one of spectrogram bands of interest (LF and HF), an iterative

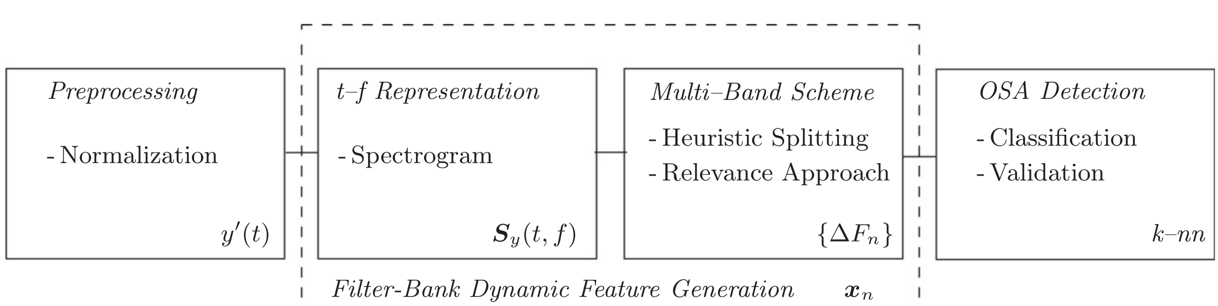

Fig. 2. Schematic representation of an automated system for OSA detection based on analysis of filter-banked dynamic features.

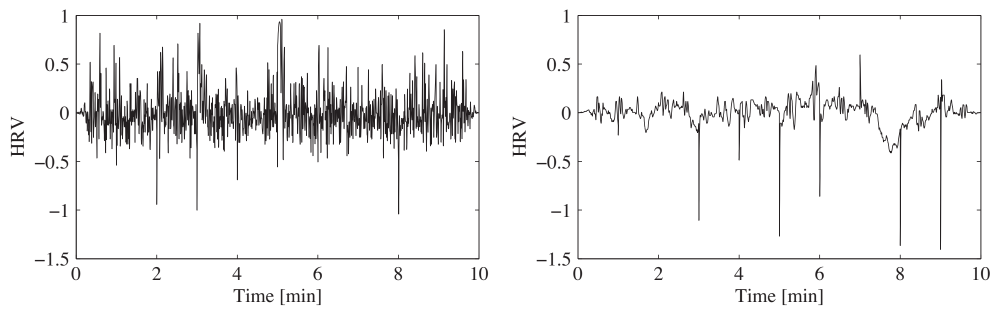

(a) normal (b) OSA

Fig. 3. Examples of 10-min segment of HRV time series labeled as normal (a) and apnoeic subjects (b), respectively.

searching process is to be carried out, which requires for an evaluation metric of every new extracted filter-banked feature. As such a measure, the average classification accuracy of OSA detection is introduced. Since the classifier optimization is out of the present study's scope, a simple *k*-nearest neighbor (*k-nn*) classifier is provided, followed by the well-known cross-validation methodology.

The heuristic approach of spectral splitting is implemented by the Algorithm 1, which produces as outcomes the number of filters n_F and the number of dynamic features p providing the maximum accuracy of OSA detection.

Fig. 5 shows the performed accuracy for searching the best combination of filter bank parameters (n_F and p). Evaluation measure of accuracy is calculated separately for each band of interest: LF (see Fig. 5a) and HF (see Fig. 5b). At this point, it can be seen that the tuning procedure of used *k-nn* classifier is not a critical step, since the attained values of accuracy are quite similar within the studied range of filter bank parameters.

As a result, a training set of $p = 10$ dynamic FCC features is achieved using triangular response filters ($n_F = 10$) with 10% overlap: the first 5 ones are regarded to the LF, and the remain 5 features are regarded to HF.

Algorithm 1. Heuristic approach-based algorithm for frequency band selection

Input: HRV time series observation set, $i \in M$
Output: Filter bank parameter set, $\{p, n_F\}$
foreach $i \leftarrow 1$ **to** M **do**
- Compute HRV signal spectrogram: $\boldsymbol{S}_y^i \in \mathbb{R}^{F \times T}$;

end
- Parameter initialization $\epsilon = 10\%$; $n_F = 2$; $n_{F max} = 20$;

while $Acc_{max} - Acc_{min} \leq \epsilon$ // $n_F < n_{F max}$ **do**
- Split the frequency axis into n_F sub–bands by means of n_F triangular response filters.
- Compute n_F dynamic FCC features.

foreach $p \leftarrow 1$ **to** n_F **do**
- Create a feature subset corresponding to the first p FCCs;
- Perform accuracy for actual feature subset by using k–nn classifier i.e. $Acc(n_F, p)$;

end
- $Acc_{max} = \max\{Acc\}$;
- $Acc_{min} = \min\{Acc\}$;
- $n_F + +$;

end
- Select the frequency bands (n_F and p) for the sub–band partition set ΔF_n, when the performed accuracy is maximized.

3.3.2. Spectral splitting based on stochastic variability

The main core of this approach is the relevance matrix calculation, given by Eq. (5). Depicted in Fig. 6 relevance matrixes of HRV spectrogram reveal a large difference in terms of dynamic behavior between both considered bands of interest. Generally, the stochastic variability contribution of every one of the stationary spectral components, measured by Eq. (6), should remain constant throughout the time axis. In this regard, neither LF band (See Fig. 6b) nor HF band (Fig. 6a) entirely hold the stationary assumption. Former relevance matrix patterns stochastic variability of spectral components with some lack of uniformity. Rather, the latter case exhibits a regular stochastic variability but within fixed time intervals, i.e, a piecewise stationary behavior might take place. From the above observations, one may confirm the difference between both HRV bands of interest in terms of stochastic properties.

Estimated values of mean and variance of vector $\gamma(f)$ for each band of interest are also shown in left side of Fig. 6a and b. Over both vector representations, the boundaries of the achieved sub-band partition set are drawn. As in the case of heuristic splitting, the proper filter bank number per each feature is empirically fixed to be one. Algorithm 2 describes the implementation of the spectrogram splitting based on stochastic variability.

Algorithm 2. Algorithm for the frequency band selection by relevance analysis

Input: HRV time series observation set, $i \in M$
Output: Filter bandwidth set ΔF_n
foreach $i \leftarrow 1$ **to** M **do**
- Compute HRV signal spectrogram: $\boldsymbol{S}_y^i \in \mathbb{R}^{T \times F}$;
- Rearrange spectrogram matrix into a vector $\in \mathbb{R}^{1 \times FT}$;

end
- Create a matrix concatenating the *t*–*f* maps vectors $\boldsymbol{\Xi}_y \in \mathbb{R}^{M \times FT}$
- Create the relevance map $\boldsymbol{G}(\boldsymbol{S}_y) \in \mathbb{R}^{T \times F}$;
- Create the relevance vector for the frequency axis $\boldsymbol{\gamma}(f) \in \mathbb{R}^{F \times 1}$;
- Obtain the local minima in the relevance vector $\min_{\forall f}\{\boldsymbol{\gamma}(f)\}$, for the sub–band partition set ΔF_n.

Table 1 summarizes the obtained optimal frequency bands for both considered approaches of spectral splitting. As a result, the whole training set holds 10 dynamic features for the heuristic case, and 7 for the spectral splitting based on stochastic variability, i.e., takin into account that each time-evolving spectral component is given by 120 samples, the achieved dynamic feature training space holds a dimension $\boldsymbol{x} \in \mathbb{R}^{10 \times 120}$ and $\boldsymbol{x} \in \mathbb{R}^{7 \times 120}$, respectively.

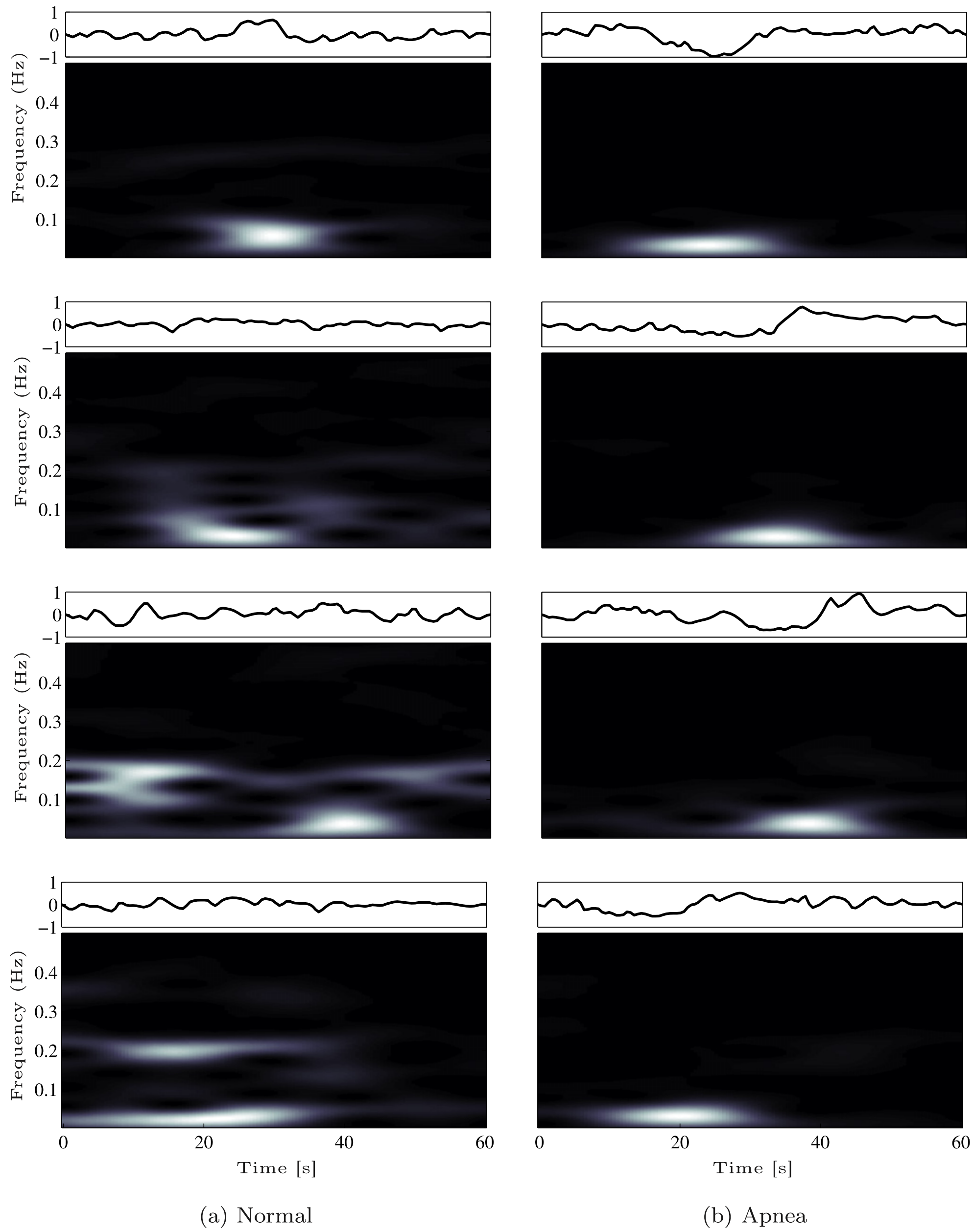

Fig. 4. Representative examples of estimated 1-min HRV spectrograms: (a) normal labeled segment and (b) apnea labeled segment.

Examples of attained filter-banked dynamic features are shown in Fig. 7 that are estimated for both spectral splitting approaches, heuristic (see Fig. 7a and b) and relevance-based (see Fig. 7c and d). Dynamic features are related to normal and apnea classes as well as to both considered bands of interest (HF and LF).

3.4. Classification performance of OSA detection

Generally, OSA detection based on HRV time series recordings is carried out in two steps (Mendez et al., 2010): (i) segment classification, and (ii) patient scoring of all-night recordings.

3.4.1. Segment classification

Throughout the following training procedures, the metric to adjust the different schemes of considered multi-band splitting is the OSA classification accuracy of each non-overlapping 1-min HRV segment, which is estimated using a simple *k-nn* classifier. Several reasons account for the widespread use of this classifier: it is straightforward to implement, it generally leads to good recognition performance thanks to the non-linearity of its decision boundaries, and its complexity is assumed to be independent of the number of classes.

Nonetheless, due to a huge dimension, which is inherent to the achieved dynamic feature training space, the *k-nn* classifier requires a high computational cost with large memory amount. So, strong dimension reduction of such large training feature set should be carried out. Since there is a need for finding feature groups that are highly correlated (as it is the case with dynamic feature-derived data), the principal component analysis is used throughout this study as unsupervised method to perform dimensionality reduction over the input training set in hand (See Section 2).

The tuning of used *k-nn* classifier is carried out by calculating the optimal number of neighbors in the sense of performed classification accuracy. For classifier testing purpose, selected training

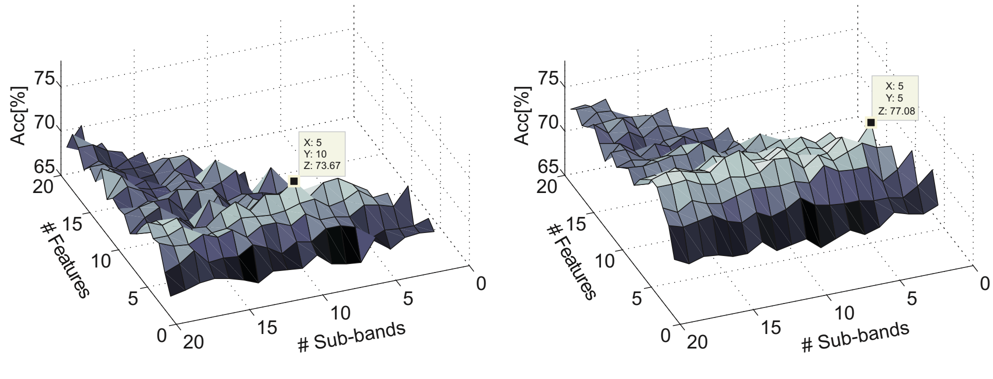

(a) LF band tuning (b) HF band tuning

Fig. 5. On calculating the optimal filter bank parameters by using classification accuracy of OSA detection.

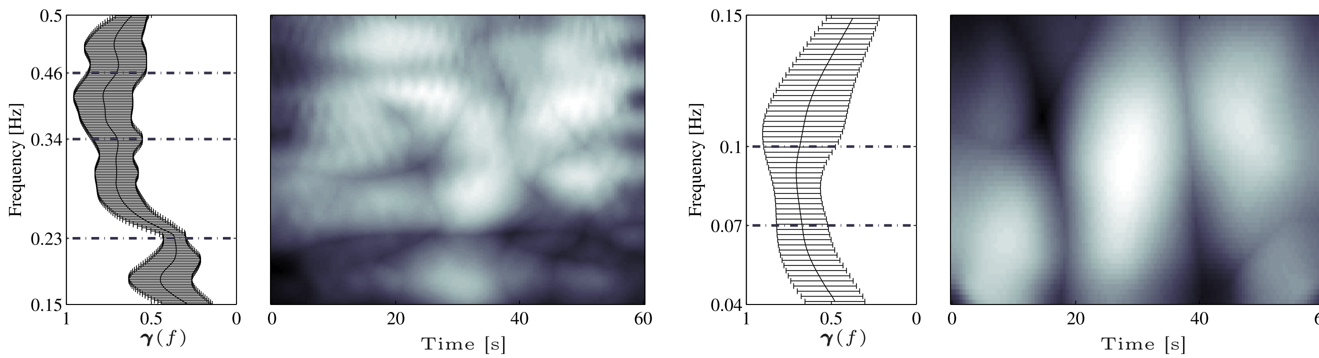

(a) HF band (b) LF band

Fig. 6. Measured relevance matrixes in terms of stochastic variability.

Table 1
Attained optimal sub-band set within the filter-banked feature extraction is carried out.

Band of interest	Approach	Sub-bands (Hz)	p
LF	Heuristic	0.04 – 0.054, 0.052 – 0.066, 0.064 – 0.078, 0.076 – 0.09, 0.088 – 0.1.	5
	Relevance	0.04 – 0.07, 0.07 – 0.10, 0.10 – 0.15.	3
HF	Heuristic	0.15 – 0.22, 0.21 – 0.29, 0.28 – 0.36, 0.35 – 0.42, 0.41 – 0.5.	5
	Relevance	0.15 – 0.23, 0.23 – 0.34, 0.34 – 0.46, 0.46 – 0.5.	4

database set holds 25 recordings coming from 13 apnoea, 4 borderline, and 8 control subjects that never had been seen during training stage. Fig. 8 illustrates the estimated performance in dependence on the number of considered principal components, which are mutually linear independent combinations of original variables, when varying the number on nearest neighbors. Performed accuracy for each one of the multi-band splitting approaches is estimated in two cases: when combining dynamic features coming from both bands of interest into a single training set, or when each band set is considered separately. In either case, an adequate number of neighbors can be adjusted to be $k = 29$, whereas the needed number of latent components is 26 to get the best accuracy values. Henceforth, those values are fixed as working *k-nn* classifier parameters for further training of both considered multi-band splitting approaches.

The classification performance is measured by means of the accuracy, sensitivity and specificity, defined by:

$$Ac(\%) = \frac{n_C}{n_T} \times 100,$$
$$Se(\%) = \frac{n_{TP}}{n_{TP} + n_{FN}} \times 100,$$
$$Sp(\%) = \frac{n_{TN}}{n_{TN} + n_{FP}} \times 100$$

where n_C is the number of correctly classified patterns, n_T is the total number of patterns used to feed the classifier, n_{TP} is the number of true positives (objective class accurately classified), n_{FN} is the number of false negatives (objective class classified as reference class), n_{TN} is the number of true negatives (reference class classified as objective class), and n_{FP} is the number of false positives (reference class classified as objective class).

Table 2 summarizes the best classification values performed over non-overlapping 1-min segments, using a single tuned 29-*nn* classifier for both considered approaches of spectral splitting. As seen,

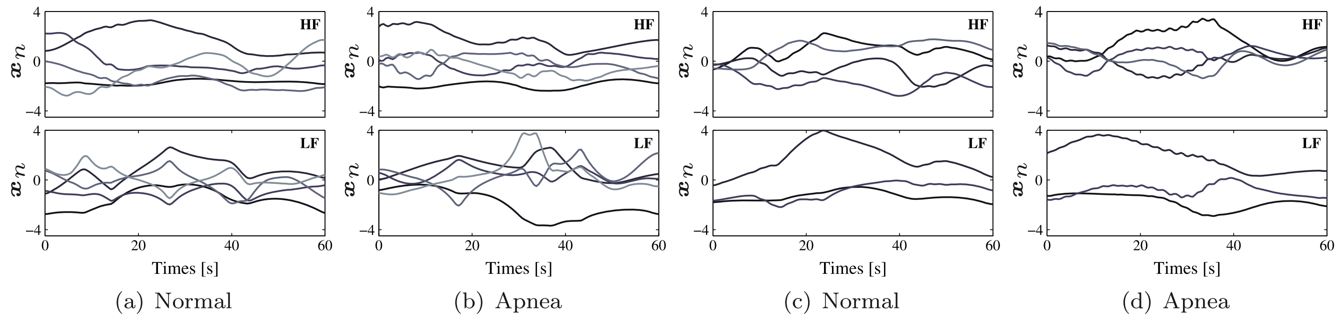

Fig. 7. Representative examples of extracted dynamic features by using both considered approaches of spectral splitting, (a) and (b) for heuristic; (c) and (d) for relevance-based.

there is no statistical difference in terms of classification performed by each one of the considered splitting approaches. In regard to each band of interest, contribution of either spectral band is alike (some close to $74-75\%$). But when considering both bands together, there is just a little improvement of the achieved classification performance ($\sim 77-78\%$).

The main reason of such a modest training contribution when gathering both bands of interest may be the observed difference between them in terms of stochastic behavior (See Fig. 6). For this reason, the parallel combining *k-nn* classifier with median selection rule is used with aim to improve the performance of the proposed approaches, thus, each dynamic feature subset is used separately. For either multi-band splitting approach, the best performance ($Ac \sim 80.6\%, Se \sim 76.2, Sp \sim 82.2$) of the combining classifier that is achieved over testing dataset is shown in Table 3. Nonetheless, some degradation of performed sensitivity on validation set is fixed that maybe explained because of the difficulty of properly labeling the apneic 1-min episodes by clinic professionals.

3.4.2. Scoring of all-night recordings

Every one recording is diagnosed to be related of either class grounded on decisions that are attained for the corresponding patient set of 1-min segments. Fig. 9 shows class separation based on OSA detection of 1-min segment within a single all-night recording (horizontal axis corresponds to the cardinal recording number). Obtained values using the parallel combining classifier are estimated for both splitting approaches: heuristic (see Fig. 9a) and relevance-based (see Fig. 9b), respectively. The circle represents the apneic subjects, the cross stands for borderline class, and the star stands for normal subjects. As seen for either splitting approach, a complete separation between normal and pathologic classes can be achieved using a minimum set of 30 apnoea segments of 1-min length per a single all-night recording. Yet, the borderline recordings are randomly located in class A or C, so their adequate interpretation remains an open issue. Therefore from achieved class separation values, both discussed splitting approaches can be implemented for OSA diagnosing.

4. Discussion

It should be remarked that the main goal of the present study is to supply a complex of signal processing algorithms for the OSA detection based on HRV recording analysis with the added benefit of simplicity and interpretability of the assessed feature set. The methodology lies on the hypothesis that using relevance-based splitting scheme over enhanced representation of HRV signals a set of dynamic filter-banked features can be extracted providing an appropriate OSA segment classification accuracy as well as high apneic patient discrimination. Although the filter-banked dynamic features extracted from biosignal recordings had been discussed previously for OSA detection (Sepulveda-Cano et al., 2011), the present study is framed on analysis of spectral splitting derived from stochastic variability of HRV time-varying spectral component set.

The obtained results evidence the following aspects to take into consideration:

(i) So far, discussed training approach for OSA detection has been tested without high restrictions on the preprocessing stage (artifact removing, denoising). Besides, attained estimation of HRV time series, which is based on QRS complex detection (Sörnmo & Laguna, 2005), provides enough accuracy, and therefore is suitable for automatizing the suggested methodology for OSA diagnosing. Nonetheless, to test and compare discussed OSA detection algorithms, it becomes necessary to extend the analysis over wider number of available dataset recordings, as quoted in (Lado et al., 2009). In this regard, the more elaborated QRS detection errors should be implemented. Specifically, ectopic beats that often occur do not reflect autonomic nervous system activity, and are to be a priori identified and discarded.

(ii) The used input time series enhancement by introducing *t–f* representations should be regarded as an important factor for adequate filter-banked feature generation. In this study, the dynamic filter-banked feature set is extracted from Fourier-based spectrogram that had been reported to be appropriate for OSA analysis (Al-Abed, Manry, Burk, Lucas, & Behbehani, 2009). As shown in Table 3, the best performed values of accuracy, sensitivity, and specificity ($Ac \sim$ 80.6%, $Se \sim 76.2$, $Sp \sim 82.2$, respectively) by proposed spectrogram-based feature set are comparable with other outcomes reached by reported OSA detection methods having simplicity of computation (Al-Angari & Sahakian, 2007). Generally, the spectrogram is desirable for signals with a slow time-varying spectrum, but suffers from the *t–f* resolution compromise. As the HRV dynamic pattern tends to be non-stationary, other nonparametric *t*Ũ-*f* representations (mostly, Wavelet Transform or Empiric Mode Decomposition) had become a powerful alternative to analyze HRV time series oriented to automatic OSA screening (Mendez et al., 2010; AH. Khandoker & Karmakar, 2009). However, some issues should be considered prior to involve other *t–f* representations within the discussed relevance-based splitting framework. Namely, the Wavelet Packet Analysis that is free of any assumptions about the stationarity of the biological signals had been used for evaluation of HRV sub-frequency regions in supraventricular tachyarrhythmia patients (Bilgin, Çolak, Polat, & Koklukaya, 2009). But, when performing the fine and coarse resolution components the resulting sub-band coefficient number

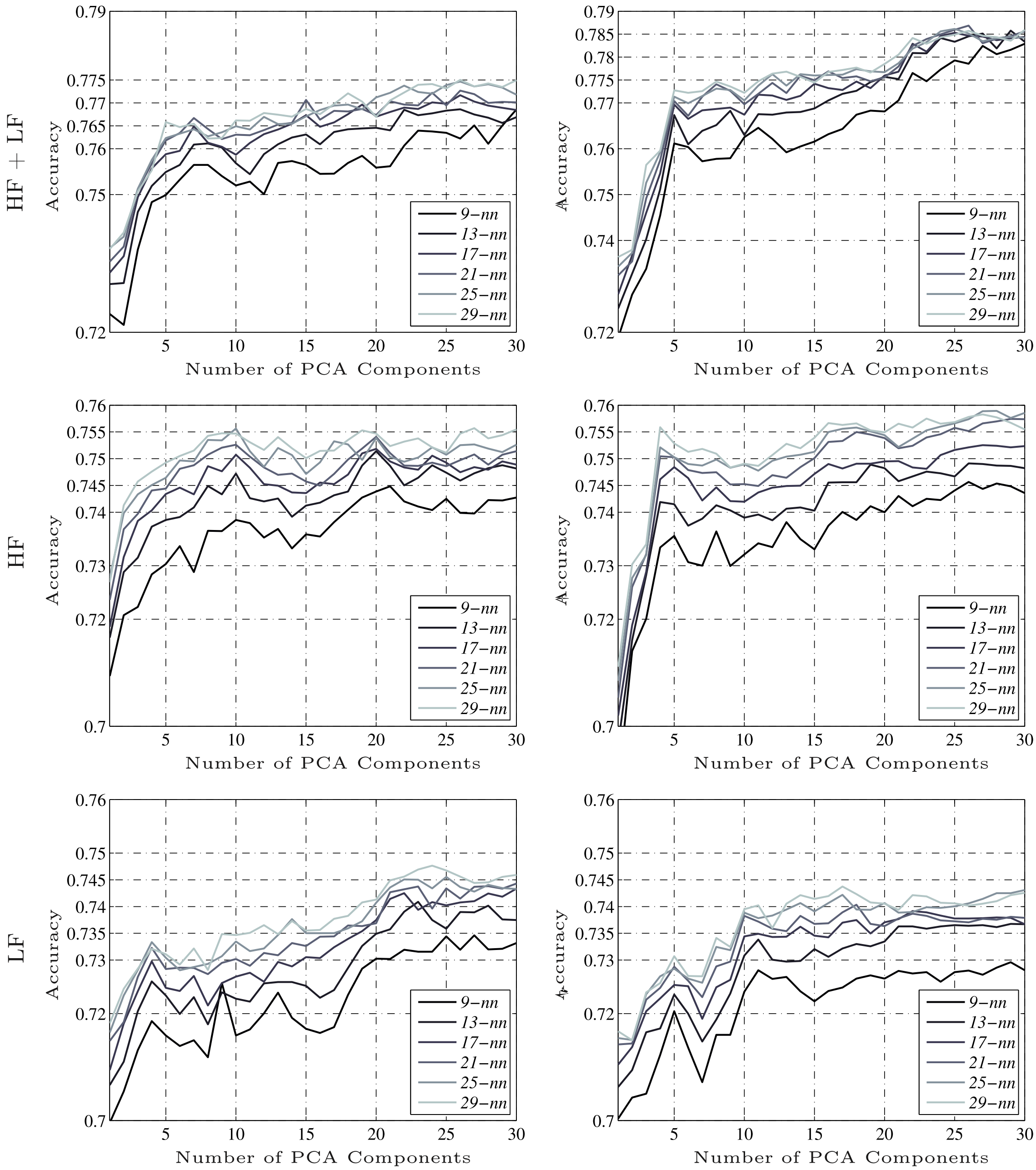

(a) Heuristic Approach (b) Relevance Approach

Fig. 8. On tuning of used *k-nn* classifier: Accuracy performance depending upon the number of neighbors when varying the number of used principal components, for both considered cases of spectral splitting.

Table 2
Performance outcomes for both approaches of spectral splitting using a single tuned *k-nn* classifier.

Approach		*Ac* (%)	*Se* (%)	*Sp* (%)
Heuristic	LF	74.76 ± 0.93	68.31 ± 1.82	78.41 ± 0.79
	HF	75.57 ± 0.85	68.73 ± 1.36	79.64 ± 1.03
	HF + LF	77.50 ± 0.95	69.25 ± 1.62	83.31 ± 0.66
Relevance	LF	74.38 ± 1.18	67.73 ± 1.72	78.09 ± 0.96
	HF	75.75 ± 0.58	69.60 ± 1.02	79.22 ± 0.84
	HF + LF	78.57 ± 0.48	71.70 ± 1.10	82.99 ± 0.76

Table 3
Best performance outcomes assessed on testing set for both approaches of spectral splitting.

	Approach	*Acc* (%)	*Se* (%)	*Sp* (%)
Training set	Heuristic	81.77 ± 0.92	82.46 ± 1.92	81.49 ± 0.95
	Relevance	81.17 ± 0.88	83.11 ± 1.59	80.38 ± 0.89
Testing set	Heuristic	80.61	76.22	82.27
	Relevance	80.19	76.44	81.54

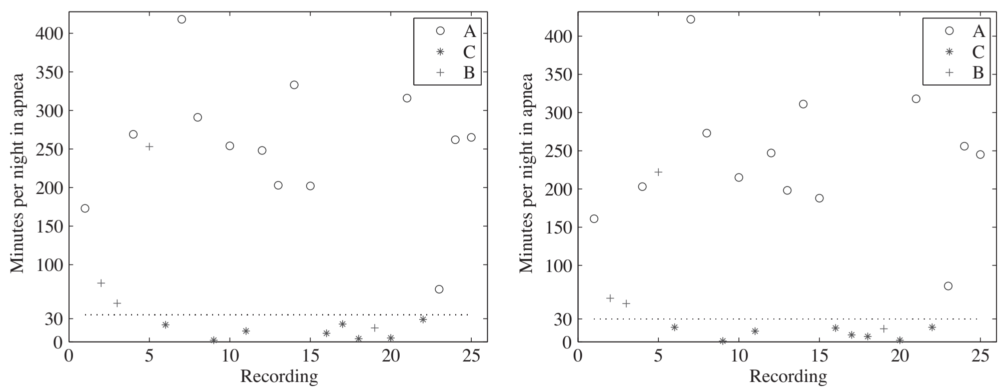

(a) Heuristic analysis (b) Relevance analysis

Fig. 9. Recording class separation for both approaches of spectral splitting.

becomes different for each node, while the proposed methodology based on the spectral splitting scheme requires for an equal number of samples per time-evolving spectral component. Likewise, the Empirical Mode Decomposition can be used, but paying attention that its implementation contains heuristic and ad hoc elements that make it hard to analyze mathematically (Daubechies, Lu, & Wu, 2011).

(iii) Several studies had established the discriminating capability of HRV activity frequency bands between normal and sleep apnoea patients (Abdullah, Holland, Cosic, & Cvetkovic, 2009), thus, the set of considered short-time measures needs to be related to the time-variant features suitable estimated by spectral sub-band methods. Namely, frequency cepstral coefficients is introduced that allow a better energy distribution identification, emphasizing the different frequency components improving OSA detection. It is worth noting that assessed feature set does not require for further processing, by instance, smooth filtering over time windows over exceeding the assumed non-overlapping 1-min HRV segment. This issue becomes important to get a well defined methodology of HRV processing, as demanded in (Lado et al., 2009). In addition, since more efforts should be done to define the features carrying fundamental information for the OSA classification, as quoted in (Mendez et al., 2010; Sepulveda-Cano et al., 2011), then the set of considered features can fulfil with this requirement because of their easier filter-banked interpretation.

(iv) Present study discusses the introduction of multi-band spectral splitting over the HRV spectrogram to optimize the performance of achieved dynamic filter-banked feature set, in terms of improving the highest OSA detection accuracy with the lowest possible complexity (fewest stochastic feature set but not increasing the computational effort). Both considered approaches of band partitioning (heuristic and relevance-based) achieve an small feature number (10 FCC parameters for heuristic or 7 for latter splitting approach). In addition, since the extracted feature set is directly related to HRV sub-bands, the discussed training methodology provides additional benefit of easier clinical interpretation of HRV-derived parameters.

(v) Since heuristic splitting approach does not take efficient advantage of the distributed information over spectrogram, the stochastic variability is introduced that measures the amount of useful information within spectral component set. As a result, the relevance matrix is achieved that determines distinctly the relevance related to each one of the spectral components along the time axis. As shown in Table 1, both obtained spectral grids are similar concerning the estimated band partition boundaries for both considered bands of interest. Detailed visual inspection of estimated relevance matrix in Fig. 1 shows that the most relevant information, for OSA detection, is the LF sub-band partition ranging from 0.07 to 0.1 Hz, as well as the HF sub-band between 0.34 and 0.46 Hz that should be related to respiratory arrhythmia. Both found relevant sub-bands can be supported by previous results obtained through different methodologies (Mendez et al., 2010; Lado et al., 2009).

(vi) Another finding from assessed relevance matrix is the observed difference between LF and HF bands of interest in terms of stochastic behavior that can lead to a modest OSA performance contribution when gathering both bands. Moreover, neither LF nor HF band entirely hold the stationary assumption. In this line of analysis, spectral splitting should be performed using relevance measures coming from nonlinear analysis of time series, by instance, the entropy as suggested in (Al-Angari & Sahakian, 2007).

(vii) Even that the classifier optimization stage is beyond the scope of the present study, to boost the HRV segment classification accuracy, a simple parallel combining *k-nn* classifier with median selection rule is used. As a result, assessed dynamic FCC feature set reaches as much as 80% value of accuracy, for both considered approaches of spectral splitting. Nevertheless, based on achieved segment accuracy, based on the minute-by-minute classification, the results showed that the two considered splitting approaches are able to separate entirely (100%) the normal recordings from the apneic ones.

5. Conclusions

A new methodology for OSA detection is explored, which is based on spectral splitting upon spectrogram representation, derived from HRV recordings. The discussed methodology, which supplies simplicity and interpretability of the assessed feature set, lies on the hypothesis that using relevance-based splitting scheme over enhanced representation of HRV signals a set of dynamic filter-banked features can be extracted providing an appropriate OSA segment classification accuracy as well as high apneic patient discrimination. Particularly, two different splitting approaches are considered (heuristic and relevance-based). In the former case, a given bandwidth of interest is arbitrary split in equally spaced sub-band partitions, whereas in the case of the relevance-based approach, searching for spectral components with alike dynamic behavior is carried out, with aim to create the sub-band partitions for the filter-banked dynamic FCC estimation, is discussed. Attained results can be oriented in research focused on finding alternative methods used for less costly and noninvasive OSA diagnosing with the additional benefit of easier clinical interpretation of HRV-derived parameters.

Nonetheless, with aim to improve the segment classification performance, some aspects should be thoroughly studied. Particularly, it would be of benefit to explore the needed enhancement by using more elaborated approaches, namely wavelet-based scalograms, matching pursuit, sparse representations, etc., in order to obtain a more accurate tracking of the strong dynamics on the HRV signals. Besides, as a future work, further efforts on testing different measures of relevance and different band selection algorithms, should be focused on extend studies to corroborate the potential of another approaches for OSA diagnosis. Lastly, the influence of different classification approaches (neural networks, hidden markov models, etc.) should be further studied to improve the performance of the proposed methodology for OSA diagnosis.

Acknowledgments

The authors would like to acknowledge M.O. Mendez for providing the needed information about the ECG data training. This work is supported by "*Centro de Investigación e Innovación de Excelencia – ARTICA*", financed by COLCIENCIAS, and "*Apoyo a tesis de posgrado – DIMA 2010*" – "*Becas para estudiantes sobresalientes de posgrado*", financed by Universidad Nacional de Colombia.

References

Abdullah, H., Holland, G., Cosic, I., Cvetkovic, D. (2009). Correlation of sleep EEG frequency bands and heart rate variability. In: *31st Annual international conference of the IEEE EMBS*. pp. 5014–5017.
AH. Khandoker, M. P., & Karmakar, C. (2009). Support vector machines for automated recognition of obstructive sleep apnea syndrome from ECG recordings. *IEEE Transactions on Information Technology in Biomedicine, 13*(1), 37–48.
Al-Abed, M., Manry, M., Burk, J. R., Lucas, E., Behbehani, K. (2009). Sleep disordered breathing detection using heart rate variability and R-peak envelope spectrogram. In: *31th Annual international conference of the IEEE EMBS*.
Al-Angari, H., & Sahakian, A. (2007). Use of sample entropy approach to study heart rate variability in obstructive sleep apnea syndrome. *IEEE Transactions on Biomedical Engineering, 54*(10), 1900–1904.
Bilgin, S., Çolak, O., Polat, O., & Koklukaya, E. (2009). Estimation and evaluation of sub-bands on LF and HF base-bands in HRV for Ventricular Tachyarrhythmia patients. *Expert Systems with Applications, 36*, 10078–10084.
Chervin, R., & Burns, J. (2011). Engineering better sleep. *Medical & Biological Engineering & Computing, 49*, 623–625.
Curcie, D., & Craelius, W. (1997). Recognition of individual heart rate patterns with cepstral vectors. *Biological Cybernetics, 77*, 103–109.
Daubechies, I., Lu, J., & Wu, H. (2011). Synchrosqueezed wavelet transforms: An empirical mode decomposition-like tool. *Applied and Computational Harmonic Analysis, 30*, 243–261.
Glass, L. (2009). Introduction to controversial topics in nonlinear science: Is the normal heart rate chaotic? *Chaos, 19*(028501), 1–4.
Haitham, M., Angari, A., & Sahakian, V. (2007). Use of sample entropy approach to study heart rate variability in obstructive sleeo apnea syndrome. *IEEE Transactions of Biomedical Engineering, 54*(10).
Kudriavtsev, V., Polyshchuk, V., & Roy, D. (2007). Heart energy signature spectrogram for cardiovascular diagnosis. *BioMedical Engineering OnLine, 6*(1), 16.
Lado, M., Vila, X., Rodríguez-Liñares, L., Méndez, A., Olivieri, D., & Félix, P. (2009). Detecting sleep apnea by heart rate variability analysis: Assessing the validity of databases and algorithms. *Journal of Medical Systems*. doi:10.1007/s10916-009-9383-5.
Mainardi, L. (2009). On the quantfication of heart rate variability spectral parameters using timeŨfrequency and time-varying methods. *Philosophical Transactions of the Royal Society, 367*, 255–275.
McMillan, D. (2002). Interpreting heart rate variability sleep/wake patterns in cardiac patients. *Journal of Cardiovascular Nursing, 17*(1), 69–81.
Mendez, M., Corthout, J., Huffel, S., Matteucci, M., Penzel, T., Cerutti, S., et al. (2010). Automatic screening of obstructive sleep apnea from the ECG based on empirical mode decomposition and wavelet analysis. *Physiological Measurement, 31*, 273–289.
Sepulveda-Cano, L., Gil, E., Laguna, P., & Castellanos-Dominguez, G. (2011). Selection of Nonstationary Dynamic Features for Obstructive Sleep Apnoea Detection in Children. *EURASIP Journal on Advances in Signal Processing, 2011*, 10.
Sörnmo, L., & Laguna, P. (2005). *Biolectrical signal processing in cardiac and neurological applications*. Elsevier Academic Press.
van Houwelingen, K., van Uffelen, R., & van Vlie, A. (1999). The sleep apnoea syndromes. *European Heart Journal, 20*, 858–866.